# CONTROL OF SINGLE-SPAN HIGHWAY BRIDGE VIBRATIONS

Thomas F. Derby and Peter C. Calcaterra, Barry Controls,
Division of Barry Wright Corporation, Watertown, Massachusetts

The investigation deals with a comparison of the dynamic response of various bridge designs to individual heavy vehicle crossings and with an evaluation of several techniques for reducing the resultant dynamic motions of long-span bridges. Four single-span bridge designs, all 250 ft in length, are considered: concrete and orthotropic composite deck constructions using both low-alloy structural steel and high-strength steel. The vibratory motions of each untreated bridge are calculated as a function of vehicle type and speed and of roadway characteristics (idealized smooth road and roadway roughness), based on simplified model representations for the bridge and vehicle. Four treatments for bridge vibration control are analyzed: rigidization, damping, passive absorbers, and active absorbers. A comparison is made between the response of the untreated and treated bridges, and the effectiveness of each treatment in reducing the dynamic motions of the untreated bridges is evaluated. Designs are evolved for each treatment, and a comparison is made on the basis of cost effectiveness. Conclusions are made regarding the dynamic response of each type of bridge design, the effectiveness of each treatment, and the choice of treatment.

•LONG-TERM trends in highway bridge design favor the construction of longer spans. Longer span bridges may be designed more economically with higher strength steels now available than with low-alloy structural steels. However, in order to realize the full economic advantage of these new materials, bridges designed with higher strength steel would be inherently more flexible.

Vibratory motions are induced in highway bridge structural members because of the passage of vehicles. In longer, more flexible spans, the magnitude of the dynamic motion may be of sufficient magnitude to result in annoying and often frightening sensations to pedestrians. In addition, increases in dynamic stress could give rise to fatigue failures. Current design specifications inhibit bridge vibrations only indirectly by controlling the stiffness of the bridge span through deflection and depth-to-span ratio limitations. These limitations have the unwanted effect of restricting the use of economical high-strength materials whose greater flexibility for a given span would not meet the present deflection requirements.

This paper considers various means, referred to as treatments, of reducing the dynamic motion of the bridge. These include rigidization, damping, and absorbers, both passive and active. The treatments should be considered as additions to the bridge structure in the event that vibration levels due to vehicle crossings are found to be excessive. In each case performance and treatment-selection criteria are developed. In addition, estimates are made of the cost associated with each treatment, and a cost effectiveness of each treatment is calculated.

## BRIDGE DYNAMIC RESPONSE

If the dynamic effects due to the interaction between the bridge and the vehicle are not taken into account, the deflection of any point on the bridge due to passage of the

Sponsored by Committee on Dynamics and Field Testing of Bridges and presented at the 50th Annual Meeting.

vehicle would be dependent only on the weight and location of the vehicle. Let the deflection at midspan of a single-span bridge due to a vehicle moving very slowly over the bridge, so as to render dynamic effects to be negligible, be called the crawl deflection. However, because dynamic effects do occur, the dynamic bridge deflection at midspan while the vehicle is on the bridge differs from the crawl deflection. The crawl deflection and dynamic deflection curves are shown in Figure 1 as a function of vehicle location. The difference between the crawl deflection and the dynamic deflection curves is referred to as dynamic increment, DI. Figure 1 also shows the residual vibration of the bridge after the vehicle leaves the span. The effectiveness of the various treatments in reducing residual bridge vibrations is discussed in another report (1).

Two characteristics of the dynamic increment are considered in the response of a bridge for a particular vehicle, speed, and roadway condition:

1. $DI_{max}$, maximum value of the dynamic increment (the vehicle location along the bridge at which $DI_{max}$ occurs is also of importance); and
2. $DI_{rms}$, root mean square value of the dynamic increment defined as

$$DI_{rms} = \sqrt{1/T \int_0^T (DI)^2 \, dt} \tag{1}$$

where T = time for vehicle to cross bridge, bridge length/vehicle speed.

## BRIDGE MODEL

The bridge is modeled as a uniform beam, simply supported at both ends, and the Bernoulli-Euler beam vibration theory with damping is used. Only the first 3 modes are considered.

The hypothetical bridges selected for this study are single-span, steel girder bridges, all 250 ft in length. This length is longer than that of the majority of steel girder bridges now in existence. Four types of bridges are considered and are labeled S-C, NS-C, S-O, and NS-O. Two of the bridges, S-C and NS-C, have concrete decks

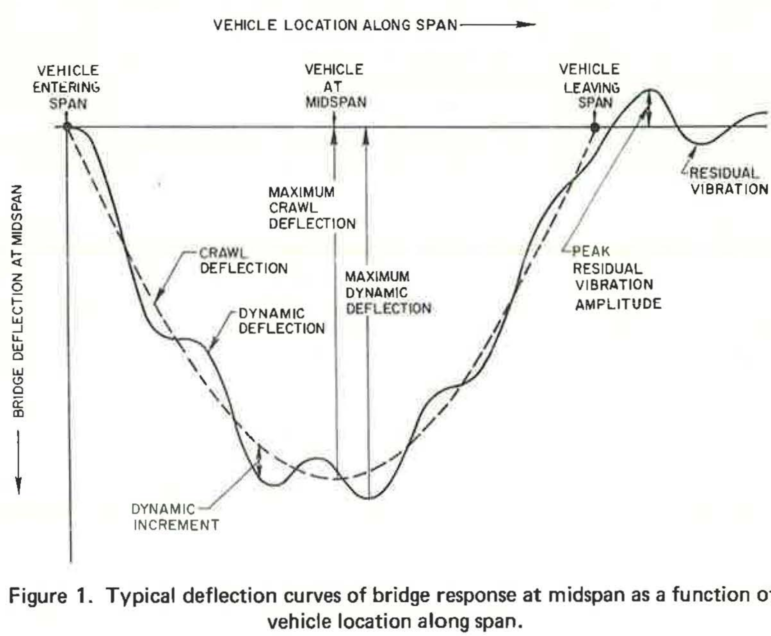


Figure 1. Typical deflection curves of bridge response at midspan as a function of vehicle location along span.

with shear connectors. One of these bridges, S-C, is built of low-alloy structural steel (ASTM A 588, design stress 27,000 psi) and meets AASHO deflection limitations. The second concrete deck bridge, NS-C, utilizes high-strength steel (ASTM A 514, design stress 55,000 psi) and does not meet AASHO deflection limitations. The remaining 2 bridges, S-O and NS-O, have orthotropic steel plate decks. One of them, S-O, is built of low-alloy structural steel and meets AASHO deflection requirements, and the other, NS-O, is built of high-strength steel and does not meet AASHO deflection requirements.

The bridges that did not meet the AASHO deflection requirements, NS-C and NS-O, also did not meet AASHO depth-to-span ratio criteria. However, all other AASHO requirements were met for all 4 bridge designs.

The sections used in all 4 bridges each consist of two 12-ft lanes and one 10-ft shoulder or 34 ft curb-to-curb with parapets on either side. All designs utilize steel girders spaced at 10.75 ft on center. In the orthotropic plate designs, it was assumed that the deck weight was 37 lb/sq ft. For bridges NS-C and NS-O, the design uses hybrid girders, that is, a low-strength, less expensive steel for the web section and a high-strength steel for the flange section. The allowable stress in the flange of the hybrid girders has been reduced in accordance with AASHO.

For the purpose of estimating the cost of the steel section, the unit prices used are as follows: web steel, A 588, 29 cents/lb; flange steel, A 588, 30 cents/lb; and flange steel, A 514, 42 cents/lb. These prices reflect the contractors bid price, complete in place. Because the costs of deck, parapets, abutments, rail, and the like would be comparable under either scheme, they are not reflected here. The properties, characteristics, and costs of all 4 bridges are given in Table 1. Typical cross sections of the concrete deck and orthotropic deck designs are shown in Figure 2.

## ROADWAY CHARACTERISTICS

The interaction between the dynamic motion of a bridge and the vehicle is complex and is influenced primarily by the characteristics of their interface, namely, the bridge deck. In addition, the vehicle enters the bridge with initial conditions that are a function of the characteristics of the approach roadway and of vehicle speed. In order to separate the effects of the vehicle weight from those of the bridge deck, 2 roadway conditions are considered in the investigation: idealized smooth road and road roughness.

### Idealized Smooth Road Condition

In order to evaluate the effect of just the vehicle weight traveling across the bridge, it is convenient to assume that both the approach roadway and the bridge deck are

TABLE 1

PROPERTIES, CHARACTERISTICS, AND COSTS OF SELECTED 250 FT LONG BRIDGES

| Bridge | Construction | Total Moment of Inertia ($in^4$) | Total Weight (kip) | Live Load Plus Impact Deflection at Midspan[a] (in.) | Natural Frequency[b] (Hz) | Web[c] (in.) | Top Flange (in.) | Bottom Flange (in.) | Steel Cost (dollars) |
|---|---|---|---|---|---|---|---|---|---|
| S-C | ASTM A 588 steel concrete deck | 4,129,288 | 1,733 | 1.91 | 1.58 | $140 \times \frac{1}{2}$ | $22 \times 1\frac{7}{8}$ | $24 \times 2\frac{1}{2}$ | 172,440 |
| NS-C | ASTM A 514 steel concrete deck | 1,891,244 | 1,555 | 4.16 | 1.12 | $110 \times \frac{9}{16}$ | $14 \times 1\frac{1}{2}$ | $18 \times 2$ | 142,520 |
| S-O | ASTM A 588 steel orthotropic deck | 2,141,416 | 979 | 3.68 | 1.52 | $157 \times \frac{9}{16}$ | $14 \times 2$ | $14 \times 2$ | 168,810 |
| NS-O | ASTM A 514 steel orthotropic deck | 588,460 | 695 | 13.38 | 0.95 | $86 \times \frac{7}{16}$ | $16 \times 2$ | $16 \times 2$ | 102,460 |

[a]Allowable live load plus impact deflection according to AASHO deflection limitation for a 250-ft bridge = 3.75 in. Live Load, HS20.
[b]First bending mode.
[c]In all cases the depth of web was determined by economy only.

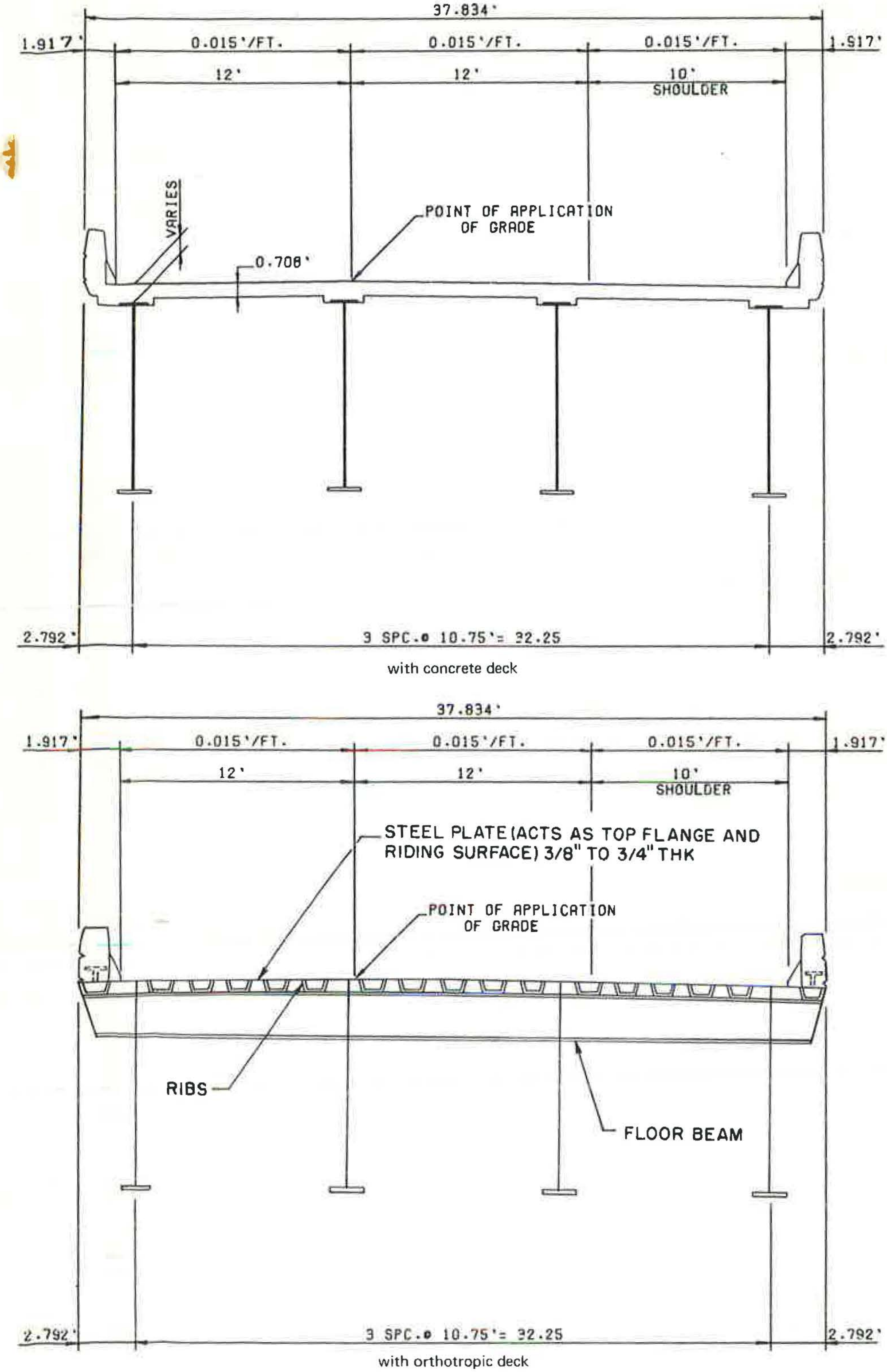


Figure 2. Typical cross sections of steel girder bridge.

"ideally" smooth. It must be emphasized that such a condition is purely a mathematical one and physically unrealizable because irregularities cannot be avoided in roadway construction. The dynamic motions that occur when a vehicle traverses a bridge under this condition (which is similar to the bridge response to a moving force of magnitude equal to the vehicle weight) represent only a portion of the total bridge response. The response under the rough road condition inherently includes the response of the bridge to the idealized smooth road condition.

## Road Roughness Condition

The most realistic condition can be considered to be one in which both the bridge approach roadway and the bridge deck have irregular profiles. The vehicle enters the span with certain initial conditions, and forced oscillations are induced on the bridge as the vehicle interacts with the structure as a result of the roughness of the deck. Therefore, for this case, the response of the bridge is the sum of these oscillations and the motions associated with the idealized smooth road response. The total response can be larger or smaller than the motions due to the vehicle weight alone, depending on phase relationships, frequency content of the deck irregularities, and frequency and speed of the vehicle.

This condition requires definition of the road profile for both the approach roadway and the bridge deck. The profile for both the approach roadway and bridge deck selected for the investigation is based on data from a "poor flexible" pavement (2) and can be mathematically represented as the sum of 20 sine functions as follows:

$$r(x) = \sum_{i=1}^{20} A_i \sin(2\pi\nu_i x + \phi_i) \tag{2}$$

where $A_i$ is the amplitude, ft; $\nu_i$ is the spatial frequency, cycles per foot; $\phi_i$ is the phase angle; and x is the distance along the bridge measured from the beginning of the span, ft. The spatial frequencies were chosen between 0.005 and 0.5 so that they would be equally spaced on log paper. The amplitudes were chosen to be proportional to $\sqrt{S_i \Delta\nu_i}$, where $S_i$ is the power spectral density at frequency $\nu_i$, and $\Delta\nu_i$ is the bandwidth for which $\nu_i$ is the center frequency. The phase angles were chosen randomly from a square distribution between 0 and $2\pi$ radians. The values of $A_i$, $\nu_i$, and $\phi_i$ are given in Table 2. In the analysis, the approach roadway and bridge deck profiles are considered to be continuous. The vehicle is assumed to have traveled over the road profile for a sufficient length of time to have achieved a steady-state motion. The vehicle then enters the bridge roadway with specific initial conditions that are a function of vehicle parameters and speed.

TABLE 2

VALUES OF AMPLITUDES, FREQUENCIES, AND PHASE ANGLES FOR ROAD PROFILE

| i | Amplitude, $A_i$ (ft) | Frequency, $\nu_i$ (cps) | Phase Angle, $\phi_i$ (radian) | i | Amplitude, $A_i$ (ft) | Frequency, $\nu_i$ (cps) | Phase Angle, $\phi_i$ (radian) |
|---|---|---|---|---|---|---|---|
| 1 | 0.0246 | 0.0056 | 2.98 | 11 | 0.0055 | 0.0565 | 0.19 |
| 2 | 0.0211 | 0.0071 | 2.78 | 12 | 0.0047 | 0.0712 | 4.74 |
| 3 | 0.0182 | 0.0089 | 3.13 | 13 | 0.0041 | 0.0895 | 3.13 |
| 4 | 0.0157 | 0.0113 | 2.34 | 14 | 0.0035 | 0.1130 | 1.53 |
| 5 | 0.0135 | 0.0142 | 5.79 | 15 | 0.0030 | 0.1420 | 0.58 |
| 6 | 0.0116 | 0.0179 | 0.78 | 16 | 0.0026 | 0.1790 | 1.76 |
| 7 | 0.0100 | 0.0225 | 0.55 | 17 | 0.0022 | 0.2250 | 1.00 |
| 8 | 0.0086 | 0.0283 | 0.25 | 18 | 0.0019 | 0.2830 | 1.33 |
| 9 | 0.0074 | 0.0356 | 2.14 | 19 | 0.0017 | 0.3560 | 0.27 |
| 10 | 0.0064 | 0.0449 | 2.95 | 20 | 0.0014 | 0.4490 | 2.41 |

## VEHICLE MODEL

For this investigation, the model chosen for the vehicle is shown in Figure 3. The suspension system is represented by a spring and viscous damper in parallel. The effect of the axle and tire mass is ignored, and the tire stiffness is represented by a spring. To completely specify the vehicle parameters, it is necessary to define the mass, the 2 spring stiffnesses, and the damping coefficient. For convenience, the vehicle parameters are expressed in terms of vehicle weight, $W_V$; damped natural frequency, $f_r$; undamped resonant frequency, $f_o$; ratio of tire stiffness to suspension system stiffness, N; and critical damping ratio, $\zeta$. For the model, the relationship between these parameters is given by

$$4\zeta^2 (8\zeta^2 - N - 2)(f_r/f_o)^6 + 16\zeta^2 (N + 1 - 2N\zeta^2)(f_r/f_o)^4 + 2 (4N\zeta^2 + N + 1)(f_r/f_o)^2 - 2N = 0 \quad (3)$$

where

$\zeta = C_V/2\sqrt{M_V K_V}$;

$f_o = \frac{1}{2\pi}\sqrt{K_V/M_V}$; and

$W_V = M_V/g$.

Justification for the model chosen and selection of vehicle parameters are based on a comparison between the road profile spectral density measured with a test vehicle over the selected poor flexible pavement and that calculated by using the vehicle model. From a report by Whittemore et al. (2), a test run was chosen for a vehicle weighing 9,400 lb, having a natural frequency of 3 Hz, and traveling at 34 mph. The profile defined by Eq. 2 and the model shown in Figure 3 with the same value of weight, natural frequency, and speed as the test vehicle were used to calculate theoretical pavement load power spectral density curves for various selected values of N and $\zeta$. Values of N = 8.37 and $\zeta$ = 2.5 resulted in the theoretical curve that best matched the experimental one. It was assumed that all vehicles considered in this study would have these same values of N and $\zeta$. On this basis, 3 vehicles were selected with different values of weight and natural frequency as shown in Figure 3. Each of the vehicles is considered to travel at three speeds: 20, 40, and 60 mph.

## DESCRIPTION OF TREATMENTS

### Rigidization

The treatment termed rigidization involves the addition of steel to the bridge to increase its stiffness. This is a rather standard procedure currently used for reducing bridge dynamic motion.

The rigidization treatments have the effect of decreasing the live load deflections by a certain percentage. Two levels of live load deflection reduction were selected for each bridge: low (approximately 25 percent reduction) and high (approximately 50 percent reduction).

The added steel is welded to the bridge in the most effective places so that a minimum amount of steel is needed for a maximum increase in stiffness; this implies that the steel is to be added to the bottom and top of existing flanges. The increase in area of these flanges is given in Table 3. Each bridge that has been rigidized will then have a new value of stiffness and a new total weight that

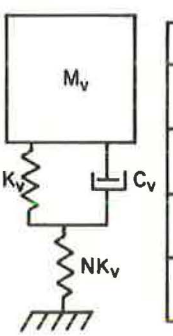


| VEHICLE CHARACTERISTICS | |
|---|---|
| FREQUENCY, $f_r$ (Hz) | WEIGHT, $W_v$ (lb) |
| 1.7 | 50,000 |
| 2.0 | 33,000 |
| 2.5 | 20,000 |

Figure 3. Vehicle model and characteristics used in this study.

TABLE 3

PROPERTIES OF RIGIDIZED BRIDGES

| Item | Low Values of Rigidization | | | | High Values of Rigidization | | | |
|---|---|---|---|---|---|---|---|---|
| | Bridge S-C | Bridge NS-C | Bridge S-O | Bridge NS-O | Bridge S-C | Bridge NS-C | Bridge S-O | Bridge NS-O |
| Design live load deflection[a], in. | 1.91 | 4.16 | 3.68 | 13.38 | 1.91 | 4.16 | 3.68 | 13.38 |
| New live load deflection, in. | 1.44 | 3.10 | 2.70 | 9.93 | 1.22 | 2.08 | 1.88 | 6.73 |
| Reduction in live load deflection, percent | 25 | 25 | 26 | 26 | 36 | 50 | 49 | 50 |
| Increase in area of girder flanges, $in^2$ | | | | | | | | |
| Top | 0 | 0 | 0 | 0 | 63.75 | 53.75 | 17 | 16 |
| Bottom | 45 | 30 | 38 | 34 | 45 | 69 | 77 | 73 |
| Total weight increase for all 4 girders, kip | | | | | | | | |
| Top | 0 | 0 | 0 | 0 | 217 | 183 | 58 | 55 |
| Bottom | 153 | 102 | 129 | 116 | 153 | 234 | 262 | 248 |
| Total | 153 | 102 | 129 | 116 | 370 | 417 | 320 | 303 |
| Midspan lower flange stress increase due to total weight of added steel, psi | 1,290 | 1,600 | 1,820 | 3,320 | 3,140 | 6,550 | 4,500 | 8,690 |
| Increase in midspan lower flange stress due to weight of added steel[b], percent | 4.8 | 2.9 | 6.7 | 6.0 | 11.4 | 11.9 | 16.7 | 15.8 |
| Total design weight of bridge[a], kip | 1,733 | 1,555 | 979 | 695 | 1,733 | 1,555 | 979 | 695 |
| New total weight of rigidized bridges, kip | 1,886 | 1,657 | 1,108 | 811 | 2,103 | 1,972 | 1,299 | 998 |
| Design total moment of inertia[a], $in^4$ | 4,129,288 | 1,891,244 | 2,141,416 | 588,460 | 4,129,288 | 1,891,244 | 2,141,416 | 588,460 |
| New total moment of inertia of rigidized bridges, $in^4$ | 5,466,488 | 2,540,837 | 2,914,468 | 792,420 | 6,452,508 | 3,776,668 | 4,178,052 | 1,168,972 |
| Design first mode natural frequency of bridges[a], Hz | 1.58 | 1.12 | 1.52 | 0.95 | 1.58 | 1.12 | 1.52 | 0.95 |
| New first mode natural frequency of rigidized bridges, Hz | 1.74 | 1.27 | 1.66 | 1.01 | 1.79 | 1.41 | 1.83 | 1.11 |

[a]Values from Table 1.

[b]Based on bridges S-C and S-O having a design stress of 27,000 psi and bridges NS-C and NS-O having a design stress of 55,000 psi.

equals the previous weight of the bridge plus the weight of the added steel. These new weights and stiffnesses are also given in Table 3. The stress increase in the existing flanges due to the added weight is calculated on the basis that the added weight of steel is a uniformly distributed dead load added to the bridge. The assumption was also made that all the steel is first clamped in place and then welded. The stress increases are given in Table 3.

Of the 2 rigidization treatments chosen for each bridge, the lower values (25 percent reduction for the concrete deck bridges and 26 percent for the orthotropic deck bridges) are considered to be feasible. The other 4 rigidization treatments are considered to be somewhat impractical because of the large amount of steel required and the high stress levels brought about in the existing flanges by the added weight. Rigidization treatments based on higher values of percentage of live load reduction also require that steel be welded to the top flanges, which is considered more difficult to perform in the field. They are included, however, to show an extreme of what could be achieved with rigidization.

## Damping

One of the methods selected as a treatment to reduce dynamic bridge motion is the addition of damping to the bridge. The amount of damping present in the untreated bridges is designated in terms of the loss factor, defined as the log decrement divided

TABLE 4

WEIGHT LIMITATIONS ESTABLISHED FOR DAMPING TREATMENTS

| | 3.7 Percent Stress Increase at Midspan | | | 7.4 Percent Stress Increase at Midspan | | |
|---|---|---|---|---|---|---|
| Bridge | Design Stress (psi) | Stress Increase Due to Weight of Damping (psi) | Uniformly Distributed Load (lb/ft) | Design Stress (psi) | Stress Increase Due to Weight of Damping (psi) | Uniformly Distributed Load (lb/ft) |
| S-C | 27,000 | 1,000 | 473 | 27,000 | 2,000 | 946 |
| NS-C | 55,000 | 2,000 | 511 | 55,000 | 4,000 | 1,022 |
| S-O | 27,000 | 1,000 | 284 | 27,000 | 2,000 | 568 |
| NS-O | 55,000 | 2,000 | 279 | 55,000 | 4,000 | 558 |

by $\pi$. All bridges are considered to have an inherent loss factor of 0.02. When a damping treatment is added to a bridge, the total loss factor is then the loss factor associated with the treatment plus 0.02.

The addition of a damping treatment to a bridge structure increases the midspan dead load stress. Therefore, the total loss factor that can be achieved for a given bridge is dependent on the weight of treatment that can be added without exceeding allowable stresses.

Two limits were established for the midspan dead load stress increase. The first limit involved a stress increase of 3.7 percent of the design stress; the second limit involved a stress increase of 7.4 percent of the design stress. The 3.7 percent limit implies a midspan stress increase of 1,000 psi in bridges S-C and S-O, which have a design stress of 27,000 psi, and a 2,000 psi stress increase in bridges NS-C and NS-O, which have a design stress of 55,000 psi. The 7.4 percent limit implies a midspan stress increase of 2,000 psi in bridges S-C and S-O and a 4,000 psi increase in bridges NS-C and NS-O. The corresponding maximum uniformly distributed loads for all these conditions are given in Table 4. The 2 stress limits for each bridge imply that 2 values of loss factor will be obtained for each bridge.

Several damping mechanisms were evaluated and "multiple-band" damping was selected for all cases in order to provide a maximum value of total bridge loss factor consistent with the limits in stress due to weight of the added material. The treatment, shown in Figure 4, consists of an alternate series of metal bands and viscoelastic material thicknesses. The metal bands are periodically attached to the primary structure to be damped. Relative motion between 2 attachment points induces shear strains in the viscoelastic material via the metal bands.

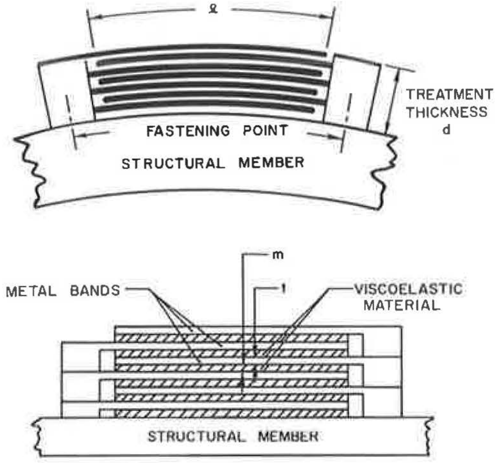


Figure 4. Schematic representation of multiple-band damping treatment.

The viscoelastic material was selected on the basis of providing an optimum peak loss factor when its properties were determined at a frequency of 1.0 Hz and a temperature of 77 F. The change of properties with frequency for a viscoelastic material implies that the loss factor of the bridge will be approximately a maximum for the first mode of vibration and will decrease with higher modes. The width of each damper is approximately 11 ft, and 3 dampers are installed side by side to cover the full width of the bridge (33 ft). The total length of the damping treatment is 250 ft. The viscoelastic material is cemented to the steel bands. In the installation, a typical 4-ft long unit is lifted into place, and the viscoelastic material and contact cement are applied to attach the unit to the previous unit placed before it. Concurrently, fasteners are welded to the bottom flanges.

Steel was selected as the material for the metal bands because it yielded values of loss factors slightly higher than those yielded by aluminum when the weight limitations were considered. The steel selected is COR-TEN "A", provided by U. S. Steel, which resists progressive rusting. The steel band thicknesses are in commercially available gage thicknesses.

## Passive Absorber

The analysis of the passive absorber considers a rigid mass attached to the midspan of the bridge by a linear spring with viscous damper in parallel.

It is desirable to have the absorber mass, $M_a$, as large as possible so that forces acting on it (and hence on the bridge) are large enough to effectively reduce bridge vibrations without resulting in large absorber deflections. However, because the bridge structure must support the absorber mass, consideration must be given to the increase in bridge stress due to the added absorber weight. Therefore, in all cases, the absorber mass was selected so that its static weight caused an increase in stress no greater than 4 percent of the design stress. The actual increase in stress was 1,000 psi for bridges S-C and S-O and 2,000 psi for bridges NS-C and NS-O. The selected values of the absorber weights are 59, 64, 35.5, and 35 kips for bridges S-C, NS-C, S-O, and NS-O respectively.

Two other parameters need to be chosen to describe the characteristics of the passive absorber: stiffness of the spring, $K_a$, and the damping coefficient, $C_a$. Values for these parameters are selected indirectly by defining the undamped natural frequency as

$$f_a = \frac{1}{2\pi} \sqrt{K_a/M_a} \tag{4}$$

and the viscous damping ratio as

$$\zeta_a = \frac{C_a}{2\sqrt{K_a M_a}} \tag{5}$$

In all cases, the undamped natural frequency, $f_a$, was set equal to the first mode bridge frequency. The viscous damping ratio, $\zeta_a$, was chosen by considering values of $DI_{max}$ and $DI_{rms}$ where $\zeta_a$ had values ranging from 0 to 0.5. A consideration of these results and the practicality of obtaining damping (i. e., it is quite common to have viscous damping ratios of 0.1 or less but rather difficult to obtain values greater than 0.1) led to a selection of a viscous damping ratio of $\zeta_a = 0.1$ for all cases.

The 3 elements that make up the passive absorber are the rigid mass, the linear spring, and the viscous damper. The rigid mass is simply composed of a block (or blocks) of concrete of proper size to make up the required mass. The linear spring is made from elastomeric material. One of the advantages of using elastomeric materials in the design of spring elements is their inherent damping capacity that ranges from $\zeta = 0.05$ to 0.1, depending on the material. If steel springs are used to generate the required stiffness values, additional damping devices would be needed to provide the necessary values of damping. Figure 5 shows the manner in which the elastomeric spring elements could be used in this application.

Becasue of molding limitations, the thickness of each pad is restricted to 3 in. Therefore, steel plates are bonded to each side of the pads, and the plates are bolted together for assembly. The total weight of the absorber and the corresponding stress increase at midspan are given in Table 5.

## Active Absorber

The analysis of the active absorber assumes that a rigid mass is attached to the midspan of the bridge by an actuator capable of applying a force to the absorber (and hence an equal but opposite force to the bridge at midspan) according to the following equation:

$$M_a\ddot{u}(s) = \left(\frac{s}{s + \omega_H}\right)^3 \left(\frac{\omega_c}{s + \omega_c}\right) G_v \dot{y}_m(s) + \left(G_{rv}s + G_{rd}\right)\left\{\left[y_m(s) - u(s)\right]\right\} \quad (6)$$

where

$M_a$ = mass of the absorber, lb-sec$^2$/in.;

$\ddot{u}(s)$ = $\mathcal{L}[\ddot{u}]$ (Laplace transform of the absorber acceleration), in./sec;

$s$ = Laplace transform variable, 1/sec;

$\omega_H$ = lead function cutoff frequency, rad/sec;

$\omega_c$ = lag function cutoff frequency, rad/sec;

$G_v$ = midspan velocity gain, lb-sec/in.;

$\dot{y}_m(s)$ = $\mathcal{L}[\dot{y}_m]$ (Laplace transform of the bridge midspan velocity), in.;

$G_{rv}$ = relative velocity gain, lb-sec/in.;

$G_{rd}$ = relative displacement gain, lb/in.;

$y_m(s)$ = Laplace transform of bridge midspan displacement, in.-sec; and

$u(s)$ = Laplace transform of absorber displacement, in.-sec.

Values of the active absorber mass for each bridge were selected in a manner similar to that used for the passive absorber; namely, an increase in bridge stress no

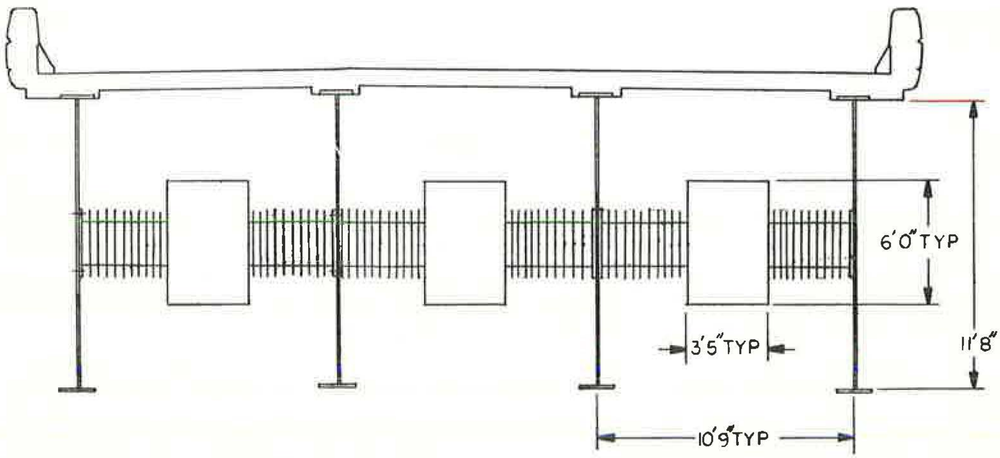


Figure 5. Typical passive absorber installation on bridge S-C.

TABLE 5

STRESS INCREASE DUE TO ADDING PASSIVE ABSORBER TO BRIDGE AT MIDSPAN

| Bridge | Weight of Inertia Block (kip) | Weight of Steel (kip) | Weight of Rubber (kip) | Total Weight (kip) | Stress Increase on Lower Flange at Midspan | |
|---|---|---|---|---|---|---|
| | | | | | psi | Percent of Design Stress |
| S-C | 59 | 13.63 | 5.49 | 78.12 | 1,323 | 4.9 |
| NS-C | 64 | 20.95 | 11.77 | 96.72 | 3,020 | 5.5 |
| S-O | 35.5 | 10.25 | 3.61 | 49.36 | 1,391 | 5.2 |
| NS-O | 35 | 17.28 | 9.10 | 61.38 | 3,505 | 6.4 |

greater than 4 percent of the design stress. The actual increase in stress was 1,000 psi for bridges S-C and S-O and 2,000 psi for bridges NS-C and NS-O. The selected values of the active absorber weights for each bridge are given in Table 6.

The active absorber acts essentially as a damper at the bridge midspan (i.e., it applies a force on the bridge, proportional but opposite in sign to the bridge midspan velocity). The gain, $G_V$, is essentially the damping coefficient. The 3 lead functions are used to attenuate low frequency components in order to avoid large deflections of the absorber. The lag function is used for stability. The relative velocity and displacement gain are used to position the absorber relative to the bridge. The values of the parameters selected for each of the 4 bridges are given in Table 6.

Because of the large masses and forces that are involved in the design of the active system, it was concluded that an electrohydraulic system could best meet the requirements of system response. Hydraulic systems are inherently among the stiffest systems available to the designer and can respond quickly and accurately to command signals.

The force acting on the absorber and, hence, on the bridge is applied by means of a hydraulic actuator connecting the absorber to the bridge. The actuator must put out a force according to Eq. 6. The oil in the actuator is assumed to be incompressible. Therefore, the flow of oil into the actuator is given by

$$Q(s) = A[\dot{u}(s) - \dot{y}_m(s)] \tag{7}$$

where Q is the flow of oil, in.$^3$/sec, and A is the piston area, in.$^2$. Combining Eqs. 6 and 7 results in an equation for the flow that will ensure that the desired force equation is satisfied. The flow can be written as a function of the bridge midspan acceleration and the relative deflection between the bridge and the absorber multiplied by shaping functions. The acceleration and relative deflection are measured with electronic transducers. These signals are fed to a servoamplifier that applies the shaping functions and puts out a signal proportional to the desired flow. The flow is delivered to the actuator by means of a hydraulic power supply and servovalve.

It is impractical to have the actuator support the weight of the absorber. Therefore, a very soft supporting spring will also connect the absorber to the bridge. Figure 6 shows a schematic representation of the active system installation.

## COMPARISON OF TREATMENT EFFECTIVENESS

This section presents a comparison of the various treatments and an evaluation of the degree of bridge vibration control that can be attained with each. Performance effectiveness is calculated for the 2 rigidization treatments, the 2 damping treatments, the passive absorber, and the active absorber for each bridge and roadway condition based on the maximum and rms values of dynamic increment. In addition, a cost effectiveness comparison is made based on values of dynamic increment and cost estimates for each treatment. The solution of the equations of motion and method of calculation are given in another report (1).

Although the vehicle travels across the span, 2 roadway conditions and 2 response criteria, $DI_{max}$ and $DI_{rms}$, can be considered to evaluate the effectiveness of each treatment in reducing bridge vibrations. Average values were calculated for each of

TABLE 6

PARAMETER VALUES FOR THE ACTIVE ABSORBER

| Bridge | $W_a$ (lb) | $\omega_H$ (rad/sec) | $\omega_c$ (rad/sec) | $G_V$ (lb-sec/in.) | $G_{rv}$ (lb-sec/in.) | $G_{rd}$ (lb/in.) |
|---|---|---|---|---|---|---|
| S-C | 59,000 | 2.48 | 9.92 | 33,400 | 1,340 | 58.7 |
| NS-C | 64,000 | 1.76 | 7.03 | 15,100 | 1,030 | 32.0 |
| S-O | 35,500 | 2.38 | 9.54 | 17,500 | 777 | 32.7 |
| NS-O | 35,000 | 1.49 | 5.96 | 4,840 | 478 | 12.6 |

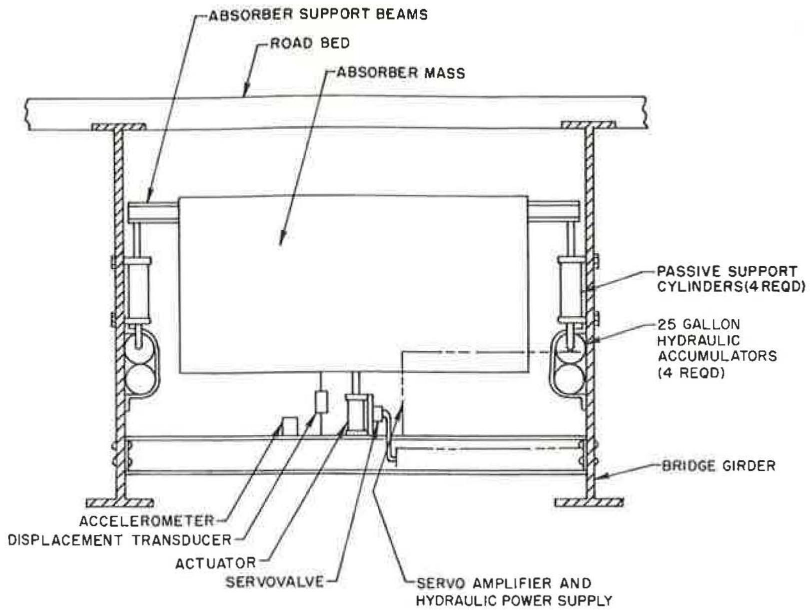


Figure 6. Schematic representation of active system installation.

the 3 vehicle velocities and the 3 vehicle types. From these data, percentage reductions were calculated comparing the treated to the untreated bridge response. These results are shown in Figures 7 through 10 for bridges S-C, NS-C, S-O, and NS-O respectively.

## Performance Effectiveness Comparison

The results shown in Figures 7 through 10 indicate that, with a few minor exceptions, there is a reasonably good correlation between the 2 criteria involving the actual

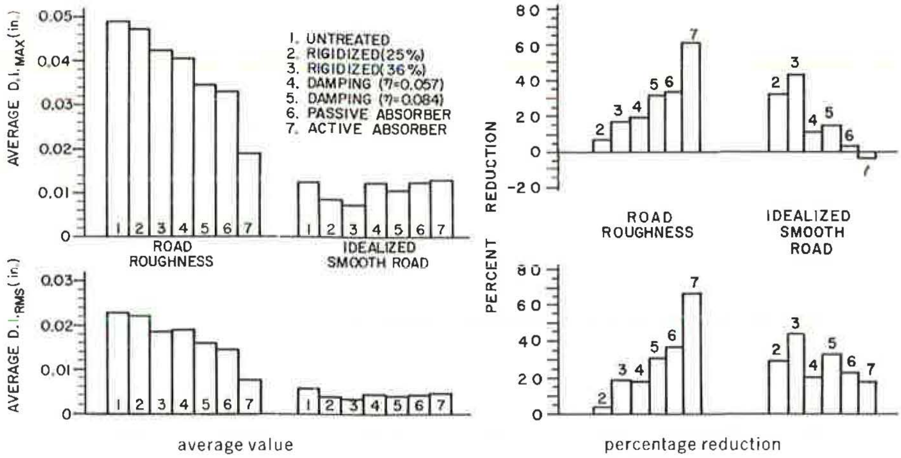


Figure 7. $DI_{max}$ and $DI_{rms}$ for all treatments on bridge S-C.

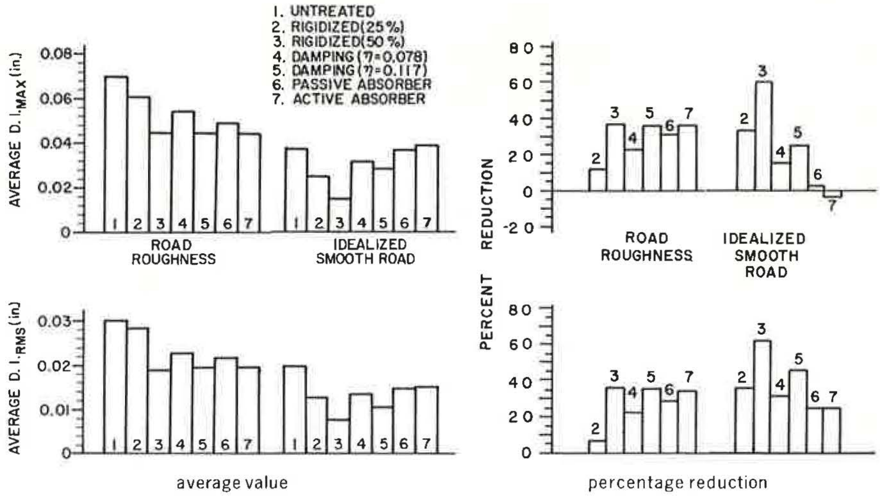


Figure 8. $DI_{max}$ and $DI_{rms}$ for all treatments on bridge NS-C.

values of $DI_{max}$ and $DI_{rms}$. These results are presented only to show the levels of midspan response with and without treatments for a particular bridge, roadway condition, and criterion. The comparison of the performance effectiveness of the various treatments is done on the basis of the percentage reduction in the response of each treatment. For each bridge type, percentage reductions are indicated for all treatments, roadway conditions, and criteria ($DI_{max}$ and $DI_{rms}$). The percentage reductions based on the 2 different criteria correlate reasonably well. Values of $DI_{rms}$ can, in a sense, be thought of as an indication of the "average" dynamic increment occurring throughout the entire travel of the vehicle along the span. Therefore, the average percentage reduction of the rms of the dynamic increment is used as a basis for comparing the performance effectiveness among treatments.

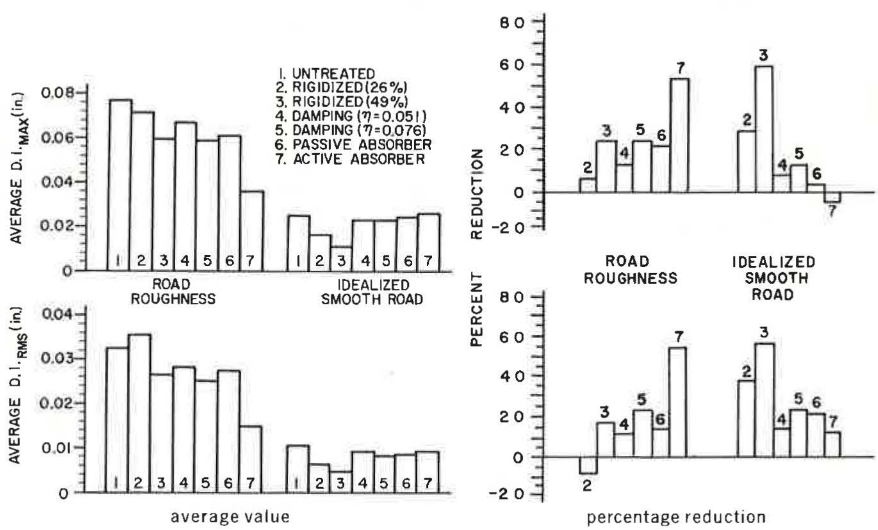


Figure 9. $DI_{max}$ and $DI_{rms}$ for all treatments on bridge S-O.

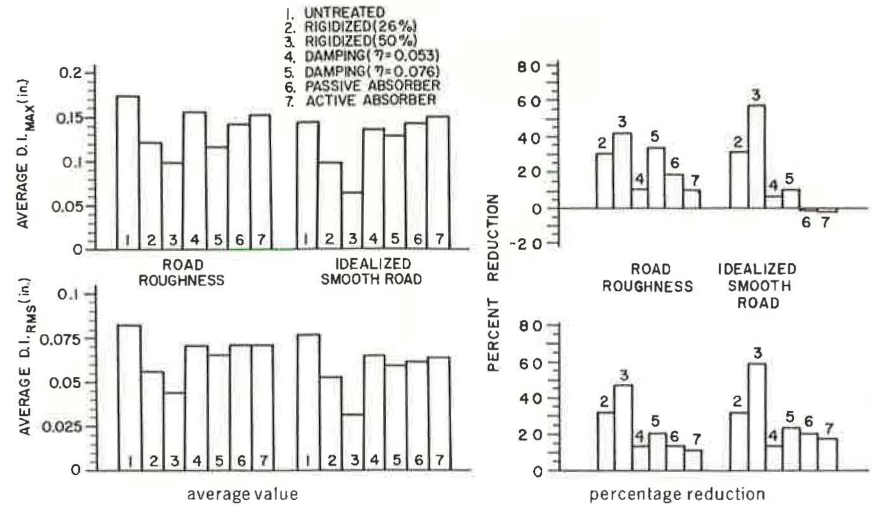


Figure 10. $DI_{max}$ and $DI_{rms}$ for all treatments on bridge NS-O.

Figures 7 through 10 show that the treatment offering the greatest performance effectiveness (or percentage reduction) differs depending on the roadway condition and bridge. As previously mentioned, the idealized smooth road condition is physically unrealizable. Bridge motions resulting from it can help in defining what portion of the total response under the road roughness condition is due to the vehicle weight.

For bridge S-C under the road roughness condition, the active absorber is most effective and the passive absorber is next best. Under the idealized smooth road condition, the high value of rigidization is best. For bridge NS-C under the road roughness condition, the high value of damping, the high value of rigidization, and the active absorber provide approximately the same percentage reduction. For the idealized smooth road condition, the high value of rigidization is the most effective. For bridge S-O under the road roughness condition, the active absorber is best; while for the idealized smooth road condition, the high value of rigidization is most effective. For bridge NS-O, the high value of rigidization provides the largest percentage reduction under both roadway conditions.

In one case under the road roughness condition (bridge S-O, low value of rigidization, Fig. 7), the interaction between the vehicle and bridge frequencies, together with the particular frequency content of the road profile, resulted in an increase in the motion of the treated bridge when compared to the untreated one (negative value of percentage reduction of $DI_{rms}$). In this instance, the oscillations due to deck irregularities are in phase with the motions induced by the vehicle weight.

## Cost Effectiveness Comparison

In addition to the treatment performance effectiveness, an important consideration in choosing a treatment is its cost. The estimated cost of each treatment is given in Table 7. For purposes of comparison, the estimated cost of steel in the untreated bridges is also shown. The determination of the treatment that gave the highest cost effectiveness was made by dividing the values of percentage reduction for the rms of the dynamic increment for each treatment by the cost of each particular treatment. The number so calculated for cost effectiveness was multiplied by $10^5$ to obtain reasonable values of a cost effectiveness index. Values of the cost effectiveness index for all treatments, bridges, and roadway conditions are shown in Figures 11 and 12 for the road roughness and idealized smooth road conditions respectively.

TABLE 7

ESTIMATED COST OF TREATMENTS

| Bridge | Untreated (steel cost only) | Rigidized | | Damping | | Absorber | |
|---|---|---|---|---|---|---|---|
| | | Low | High | Low | High | Passive | Active |
| S-C | $172,440 | $59,400 | $138,000 | $54,914 | $73,941 | $23,000 | $105,000 |
| NS-C | 142,520 | 52,300 | 185,400 | 55,930 | 71,955 | 36,000 | 110,000 |
| S-O | 168,810 | 52,200 | 123,000 | 43,013 | 64,058 | 18,000 | 99,000 |
| NS-O | 102,460 | 57,600 | 142,140 | 43,013 | 57,000 | 30,000 | 102,000 |

| BRIDGE TYPE | S-C | NS-C | S-O | NS-O |
|---|---|---|---|---|
| 2. RIGIDIZED | 25% | 25% | 26% | 26% |
| 3. RIGIDIZED | 36% | 50% | 49% | 50% |
| 4. DAMPING $\eta =$ | 0.057 | 0.078 | 0.051 | 0.053 |
| 5. DAMPING $\eta =$ | 0.084 | 0.117 | 0.076 | 0.076 |
| 6. PASSIVE ABSORBER | | | | |
| 7. ACTIVE ABSORBER | | | | |

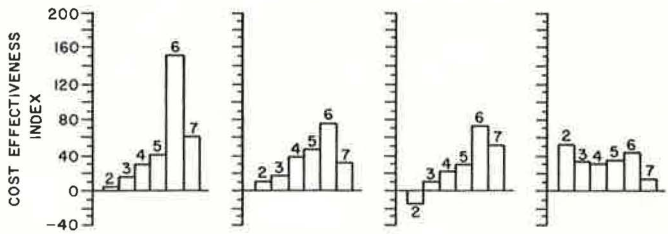


Figure 11. Cost effectiveness for all treatments and bridges based on bridge response to road roughness condition.

| BRIDGE TYPE | S-C | NS-C | S-O | NS-O |
|---|---|---|---|---|
| 2. RIGIDIZED | 25% | 25% | 26% | 26% |
| 3. RIGIDIZED | 36% | 50% | 49% | 50% |
| 4. DAMPING $\eta =$ | 0.057 | 0.078 | 0.051 | 0.053 |
| 5. DAMPING $\eta =$ | 0.084 | 0.117 | 0.076 | 0.076 |
| 6. PASSIVE ABSORBER | | | | |
| 7. ACTIVE ABSORBER | | | | |

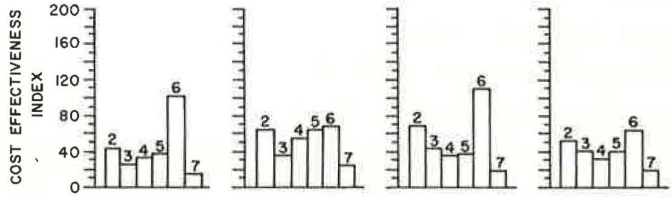


Figure 12. Cost effectiveness for all treatments and bridges based on bridge response to idealized smooth road condition.

Figure 11 shows that, for the road roughness condition, the passive absorber yields the highest cost effectiveness on bridges S-C, NS-C, and S-O. On bridge NS-O, the low value of rigidization provides the highest cost effectiveness. Figure 12 shows that, for the idealized smooth road condition, the passive absorber yields the highest values of cost effectiveness for all bridges.

Care should be exercised in using the cost effectiveness indexes to reach conclusions regarding any of the treatments. For example, the high values of cost effectiveness indicated for the passive absorber are due mainly to its low cost and not to its high performance effectiveness. Also, it must be realized that the cost figures are only estimates and would not necessarily apply to any particular bridge.

## CHOICE OF TREATMENT

A decision as to which type of treatment to use based on the reduction in $DI_{rms}$ would have to consider the type of bridge and the nature of the roadway. This study has dealt with 4 specific bridge designs and 2 roadway conditions, one of which (idealized smooth road) cannot be attained in practice because it assumes a mathematically or ideally smooth roadway on the bridge. It would seem reasonable to base the choice of treatment on the road roughness condition. However, it must be emphasized that an infinite variety of road roughness conditions actually exist in the field, that are greater or lesser in magnitude than the one chosen in this study. In addition, actual roadways may have a significantly different frequency content. If the roughness of the actual roadway is not severe, the results based on the idealized smooth road condition could be used to select the suitable treatment. On the other hand, the field roadway profile may be worse than the road roughness selected for this study. Such a case does not necessarily imply that the actual bridge roadway would be visually rougher, but rather that some characteristics of the spatial frequency content of the actual road may result in a different level of treatment effectiveness than those shown here. Therefore, in order to select an appropriate treatment based on the results presented here, it is necessary to determine which of the 2 roadway conditions is more representative of the response of a particular bridge.

The magnitude and characteristics of the bridge response to the idealized roadway condition can be shown to be closely approximated by the first mode response occurring when the vehicle is replaced by a traveling force of constant magnitude whose value is the weight of the vehicle. An approximate expression for the first mode dynamic increment of a uniform beam under a moving force of constant magnitude is given as follows (3):

$$DI = \alpha Y_{st} e^{-\pi \eta_1 f_1 t} \sin 2\pi f_1 t \tag{8}$$

where

$\alpha$ = speed parameter, $(V/2\ell)/f_1$;

$Y_{st}$ = midspan static deflection, $F\ell^3/48EI$;

$V$ = velocity of moving force;

$\ell$ = length of span;

$F$ = magnitude of concentrated force at midspan;

$EI$ = flexural stiffness of span;

$f_1$ = first mode frequency of span; and

$\eta_1$ = loss factor of span for first mode.

According to Eq. 8, (a) the maximum dynamic increment due to a moving force of constant magnitude always occurs at the first quarter-cycle of bridge motion or when the force has just entered the span; (b) the dynamic increment decreases exponentially because of damping in the span; (c) the maximum dynamic increment is directly proportional to both the speed and the magnitude of the moving force; and (d) the frequency of oscillation of the dynamic increment is the first mode frequency of the bridge.

For the low values of loss factor assumed for the untreated bridges ($\eta_1 = 0.02$), the maximum dynamic increment for a moving force may be closely approximated by

$$DI_{max} = \alpha Y_{st} \tag{9}$$

Values of maximum dynamic increment were calculated by using Eq. 9 for all vehicle speeds, force, and bridge frequencies. Good correlation was found between the calculated values based on a moving force and the corresponding computed values for the vehicle traversing the idealized smooth road.

The expression for the rms of the dynamic increment for a moving force is given by

$$DI_{rms} = \sqrt{1/T \int_0^T (DI)^2 dt}$$

$$= \alpha Y_{st} \sqrt{1/T \int_0^T e^{-2\pi\eta_1 f_1 t} \sin^2 2\pi f_1 t \, dt} \tag{10}$$

where $T = \ell/V$.

Values of the rms of the dynamic increment were calculated by using Eq. 10 for all values of speed, force, and bridge frequencies. The correlation is good, although not quite as good as was the case for the values of maximum dynamic increments. The values of the rms of the dynamic increment computed for the vehicle traversing the idealized smooth road are slightly lower than the values calculated by using Eq. 10. This is considered to be due to the vehicle acting as a vibration absorber as it undergoes a small amount of springing.

For the long-span bridges considered in this study, the parameter $\alpha Y_{st}$ provides a measure of the level of dynamic increment that will occur for the idealized smooth road condition for a given vehicle and speed. The actual dynamic increment may be different from that indicated by this parameter because of the fact that bridge approach and deck roadways are never ideally smooth. Road roughness or bumps will induce additional oscillations, and this dynamic motion may reinforce or cancel the response under the idealized smooth road condition because of the weight of the vehicle alone. Nevertheless, the calculation of the level of idealized smooth road response by the use of the parameter $\alpha Y_{st}$ is considered worthwhile. The actual level of dynamic motion indicated by field tests, when compared to $\alpha Y_{st}$, would provide an indication of the effect that roadway roughness has on the total dynamic motion. If, for a statistically significant number of field tests, the actual dynamic motion is much greater than that indicated by $\alpha Y_{st}$, then a treatment can be selected based on the results for the road roughness condition. If, however, the actual dynamic motions for a sufficient number of test vehicle runs are of the order of magnitude that would be predicted by the use of $\alpha Y_{st}$, then treatments of choice would be as indicated under the idealized smooth road condition.

## CONCLUSIONS

Based on the results presented in this report, the following conclusions can be made:

1. The large dynamic motions associated with bridges employing higher strength steels can be reduced to the levels associated with bridges employing low-alloy steels by means of appropriate treatments.

2. A technique is provided to select vibration control treatments, which on the average reduce the midspan dynamic motions of long-span bridges from 20 to 40 percent when compared to the untreated bridges. However, care must be exercised in selecting appropriate treatments because no single treatment was found equally effective for all cases considered. Also, the analysis indicates that, depending on the character-

istics of deck irregularities, use of a treatment may actually result in a larger bridge response for certain combinations of vehicle speed and weight.

3. Different values of treatment effectiveness were obtained contingent on whether the bridge deck is considered to be mathematically smooth (idealized smooth condition) or to have an irregular pavement (road roughness condition). A parameter can be calculated to approximate for the untreated bridge the level of dynamic increment that will occur under the idealized smooth road condition (constant traveling force). A comparison between calculated and measured values of this parameter can define whether results based on this condition can be used to select the most effective treatment for vibration control.

4. If field measurements of the untreated bridge indicate that the dynamic motions are primarily due to the constant traveling force, then reducing the rms level of road profile will have very little effect on the bridge dynamic motions.

5. The choice of the treatment to be applied to a bridge whose dynamic motion is unsatisfactory must be based not only on the particular bridge properties but also on the nature of the roadway. Specifically, some measure must be obtained as to the degree of influence that the level of road roughness exerts on the total dynamic response. In addition, the choice of a treatment must consider the actual amount of reduction achievable with that treatment, its cost, and whether that level of reduction is sufficient.

## ACKNOWLEDGMENT

This paper is based on results of an investigation conducted under a contract with the Federal Highway Administration.

## REFERENCES

1. DesMarais, D. A., Derby, T. F., and Calcattera, P. C. Feasibility Study of Methods, Materials and Devices for Controlling Bridge Vibrations. Barry Controls, Division of Barry Wright Corp., Watertown, Mass., final report, June 1970.
2. Whittemore, A. P., et al. Dynamic Pavement Loads of Heavy Highway Vehicles. NCHRP Rept. 105, Oct. 1970.
3. Inglis, C. E. A Mathematical Treatise on Vibrations in Railway Bridges. Cambridge Univ. Press, London, 1934.